3. Nature of Glasses

Punit Boolchand, Matthieu Micoulaut, and Ping Chen

Abstract Glasses exist in *three* generic elastic phases: *flexible*, *intermediate* and *stressed-rigid,* which are determined by the connectivity of their backbones. Measurements of glass transition temperatures (T_gs) using modulated-differential scanning calorimetry permits distinguishing these phases by their characteristic non-reversing enthalpies (ΔH_{nr}) at T_gs. In Raman scattering, characteristic elastic power-laws are observed in *intermediate* and *stressed-rigid* phases. Liquid fragilities are found to correlate with ΔH_{nr} terms in covalent networks but not in modified oxide or H-bonded networks. In the latter systems weak network links exist, which cease to constrain networks as the temperature $T > T_g$ and viscosities plummet. *Intermediate phase glasses* are composed of rigid but unstressed networks that are in a state of *quasi-equilibrium* and age minimally. Such glasses usually form space filling networks and are structurally *self-organized*.

3.1 Introduction

Most liquids upon cooling crystallize when their temperature is lowered below their melting temperature (T_m). But some liquids can bypass crystallization and become solid at a lower temperature T_g (glass transition temperature) to form a *glass*. Basic challenges about glasses have confronted materials scientists, physicists, chemists, geologists and engineers alike for over fifty years - such as: what is special about glass-forming liquids and what determines the glass transition temperatures? Are glass network structures usually random and fully polymerized [1]? In this chapter we review the remarkable progress which has taken place on the subject in the past few years both in theory and experiment. Although glass formation occurs over a very small part of phase (i.e., composition) space, it is remarkable that the phenomenon spans liquids possessing a wide range of chemical bonding. Covalent, ionic, superionic, metallic, organic polymers and bio-polymers can each exist in a glassy state. Once formed, some glasses appear to be generally quite robust and are used today in several mature technologies which require long-term stability. These observations are all the more puzzling given that glasses are intrinsically *non-equilibrium solids* (supercooled liquids), and most tend to continuously evolve with time, i.e., they age. In microelectronics, a 3-terminal

MOSFET device forms the heart of all solid state chips in circuits and systems. The gate oxide is a thin overlayer of *glassy* SiO_2 on an active crystalline Si medium. These devices routinely operate for over 10^9 cycles without degradation of the gate oxide insulator. How can that come about? The very special role of the Si-SiO_2 interface in microelectronics has come to the fore in recent years as attempts to replace the silica gate material with high- K (dielectric constant) oxides (HfO_2, ZrO_2) in aggressively scaled devices have met with utter failure. We have recently come to realize that the Si-SiO_2 interface is rather special in that it forms a *self-organized stress-free* structure [2]. The recognition has opened a new avenue to engineer high dielectric constant (high-K) gate dielectrics on the self-organized Si-monoxide layer with remarkable success [3]. Another example of a functional glass is window glass which is an empirically engineered alloy of silica, lime and soda. In an early form, glass [4] has shaped human civilization since the times of the Phoenicians and it continues to do so at present as well. It has found applications in windows of houses and churches, in arts and crafts, in the evolution of experimental science, and variants of window glass are now used in state of the art fiber optics, lenses, microscopes, cars and flat- panel displays. Window glass is a remarkably robust material and our recent understanding reveals that this is not an accident. By tuning the soda to lime ratio, one can cooperatively drive the ternary alloy to *self-organize* [5]. A number of other network systems adapt and reconfigure their structure to *self-organize*; for example, covalent network glasses [6, 7], computational phase transitions [8], high temperature superconductors [9], H-bonded alcohols and saccharides [10], and protein folding [11].

Just now we are beginning to understand how disordered networks *self-organize* [12, 13] to form systems that exist in a state of supercooled *quasi-equilibrium*.

The present volume is dedicated to phase change materials that are used in re-writable DVDs or CDs (Chapters 11 and 12), Phase Change Random Access Memory (PCRAM) devices (Chapters 13-16), as well as in potential new applications such as reconfigurable logic (Chapter 17). The technology utilizes [14] amorphous thin-films of alloys of the group IV and group V elements with Tellurium. Films of interest include $Ge_2Sb_2Te_5$ [15], which broadly form covalently bonded networks and are poor glass formers. Their networks may even be intrinsically nanoscale phase separated or demixed, i.e., composed of more than one type of a backbone structure. The interaction of light and independently heat permits films to switch locally between their amorphous and crystalline state as a group of atoms shuffle reversibly and repeatedly between the ordered and disordered state. The underlying structure changes have attracted recent interest [16] because of the commercial implications of the technology. It is thus appropriate that ideas on glass formation and structure, and particularly the nature of glass transition in covalently bonded solids be reviewed in this context. Many of the ideas on glass structure developed on Se- and S-based systems in this review will be relevant to Te-based systems as well. However, one must remember that Te-rich melts are usually semi-metallic with Te taking on a coordination number of greater than 2,

which has the consequence that it is usually not feasible to obtain melt-quench glasses in Te-rich melts. Vapor deposition is the preferred method to obtain amorphous thin-films of the tellurides. The propensity of Te cations to easily switch their coordination number between 2- to 3- or even quasi 6-fold from the amorphous to the crystalline state by a heat pulse or light flux is the functionality of interest in their applications as phase-change materials (Yamada et al. 1990).

3.2 Thermodynamics of the Glass Transition

Cooling of a liquid leading to crystallization is schematically illustrated in Fig. 3. 1, in which thermodynamic variables such as enthalpy (H), entropy (S) and molar volumes (V) undergo a first order change near T_m. Alternatively, a glass forming liquid can be supercooled below T_m and displays a higher order transition to a glass state near T_g (~2/3 T_m). Many years ago, Kauzmann [17] visualized the glass transition as an event that circumvents the entropy crisis that would result if the liquid entropy S_{liquid} continued to decrease linearly as T is lowered to the Kauzmann temperature T_K (Fig. 3.1) to become less than the crystal entropy $S_{crystal}$. Trajectories of two glass forming liquids cooled at different rates are shown in Fig. 3.1 as well; glass a (glass transition T_{ga}) is realized when a liquid is cooled at a high rate, and glass c (glass transition T_{gc}) is realized when it is cooled at a low rate. A higher cooling rate kinetically shifts the glass transition to higher temperatures, i.e., $T_{ga} > T_{gc}$. We also show the effect of aging glass a below its T_{ga}; its enthalpy H decreases (trajectory b) with time in relation to the as quenched (trajectory a) glass. Aging generally leads networks to compact as molar volumes, enthalpies and entropies decrease. The aging process involves relaxation from local metastable configurations produced by the particular quenching history. This will lower the entropy and allow a more efficient use of space.
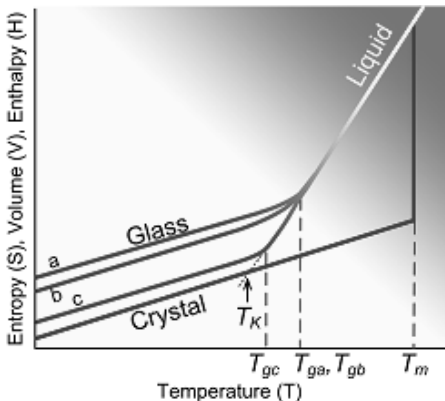
Fig. 3.1. Normal liquids crystallize at T_m, and glass forming liquids form a glass. Trajectory a and c show quench rate effects, while a and b aging effects. T_K represents the Kauzman temperature. Adapted from [18].

Historically, glass transitions are discussed within theories that emphasize the kinetic aspect [19] of the underlying process. Good glasses form even when liquids are cooled very slowly (1°C/min). Aspects of network structure [20, 21], particularly connectivity, determine the magnitude of T_g as well as the nature of glass transitions [22].

The large reduction in T_g of SiO_2 glass from 1200°C to nearly 600°C upon alloying a few mole percent of soda was known as early as 1500 BC. These large changes in T_g brought about by chemical alloying far exceed those brought about by quench rates. Currently, we do not have a theory of the glass transition to account for all these effects. Not surprisingly, Anderson [23] noted several years ago that, "the deepest and most interesting unsolved problem in solid state theory is probably the theory of the nature of the glass transition; this could be the next breakthrough in the coming decade….".

Changes in the *nature* of T_g brought about by chemical alloying can produce far more spectacular effects than hitherto recognized. The motional arrest which takes place during the glass formation and in the reverse process during melting can be thought of as involving two components: the first, which we will call *non-ergodic* (or *T*-irreversible) involves the progressive restriction of allowed structures and loss of configurational entropy, and the second, the continuous change in vibrational specific heat at each configuration, which we will call *ergodic* (or *T*-reversible). Glass formation has its roots in non-ergodic behavior. Up until recently we have not had a clear experimental handle on separating these two types of processes that underlie the glass transition. With the advent of modulated Differential Scanning Calorimetry (m-DSC), one is now in a position [22] to separate these two fundamentally different behaviors. These experiments have led to the exciting discovery of compositional *windows of almost reversible* glass formation. Taken together with other remarkable features presented in this chapter of glasses in these composition windows, they represent a *new* phase of network solids, which has come to be known as the Intermediate Phase (IP).The sharpness of *reversibility windows* in composition space, and the quasi-equilibrium nature of network structures in these windows justifies the use of the term IP. These structures, neither random nor crystalline, are thought to be of a variety known as *self-organized.* The IP is a novel phase of condensed matter, and is probably one of the select few to be discovered since polymers in the early 1920s. The experimental landscape supported by numerical simulations reveals the existence of 3 generic classes of glasses based on the elastic response of their networks, f*lexible*, *intermediate* and *stressed-rigid*. In addition to the thermal method (modulated DSC), vibrational spectroscopies (Raman scattering and infrared reflectance) have proved to be rather insightful in elucidating these phases. The latter have permitted characteristic elastic power-laws to be measured in the intermediate and stressed-rigid phases, which are supported by theory. We begin by discussing the nature of glass transitions in these phases next.

3. 3 Glass Transition from Dynamics

Insights into the glass transition have also come from the dynamic response of glass-forming liquids [24]. In supercooled liquids changes of structure with temperature are small but those in dynamical properties are large. Viscosity (η) through the Maxwell relation, $\eta = G_\infty \tau$, where G_∞ is the high frequency shear modulus and τ the shear-stress relaxation time, is a probe of liquid dynamics. At high T ($> T_g$), glass-forming liquids have low viscosities (η) and short relaxation times (τ) of the order of atomic vibrations (10^{-12} sec). Upon cooling to $T \sim T_g$, liquid viscosities increase by orders of magnitude (Fig. 3.2).
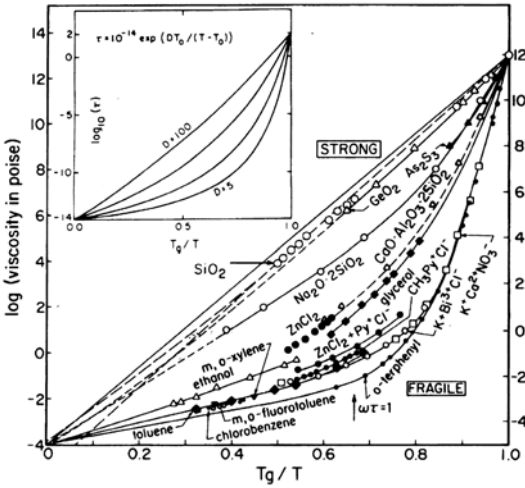
Fig. 3.2. Log of the viscosity as a function of the inverse temperature for different glass-forming liquids. The slope at T=T_g serves to define the fragility index m. Adapted from [26].

In covalent systems (such as silica or chalcogenides), changes in $\eta(T)$ are moderate and follow an Arrhenius-like behavior

$$\eta = \eta_0 \exp[\Delta E_A / k_B T] \tag{3.1}$$

Here ΔE_A represents the activation energy for viscosity, k_B is the Boltzman constant, and η_0 the high temperature limit of η. In liquids possessing softer interatomic interactions (ionic, van der Waals), $\eta(T)$ increases by several decades over a small T- range, a behavior first described by Vogel, Tamman, Hesse and Fulcher [25] in the form:

$$\eta = \eta_0 \exp[\Delta E_A / k_B (T - T_0)] \tag{3.2}$$

Here T_0 is the temperature at which η diverges and is also identified with the Kauzmann temperature T_K (Fig. 3. 1). By convention, the "dynamic" T_g is defined as the T when η acquires a value of 10^{12} Poise. This usually corresponds to the T at which the time needed to equilibrate the system becomes of the order of the timescale of an experiment (100 s), and correlates fairly well with "calorimetric" T_g. For $T < T_g$, relaxation times increase astronomically and liquids freeze into glassy solids. At $T \sim T_g$ a glass has the viscosity of a solid, but has a measurable diffusion constant which allows for a moderate relaxation on a reasonable experimental time scale. As a consequence, aging is manifested in thermal and dynamical properties, usually measured as a function of waiting time [27] after samples are synthesized by either a melt-quench or evaporation In Fig. 3.2, liquids such as SiO_2 or GeO_2 , which display an Arrhenius T-variation of viscosity are recognized as *strong*, while liquids such as o-terphenyl, glycerol and toluene, which display a bowed T-variation of viscosity leading to a high slope or activation energy near T_g are termed as *fragile*. Glassy behavior is also realized in colloids or soft sphere liquids by jamming [28]. The latter occurs when a system develops extremely long stress relaxation times in a disordered state.

To summarize, glassy behavior is realized either by increasing density of a liquid (jamming effect), by shearing [29], or by super-cooling a liquid. The nature of atomic interactions usually determine relevant parameters upon vitrification: kinetic factors in soft sphere or organic supercooled liquids, structural factors in covalent glass-forming liquids, and increase of η results when chemical bonds form between atoms.

3.4 Glass Forming Tendency

From the point of view of the configuration space of a system of N atoms, crystalline structures occupy a very small region because, on average, the atoms in one unit cell define the entire structure. This simplification begins to break down near, say, a melting transition where there is a significant number of thermally activated defects. Insight into glasses and the glass transition is challenged by the need to consider much larger regions of the configuration space. The *potential* energy of all possible configurations, defined over the 3 (or 6 including rotations)N dimensional hyperspace, is called the potential energy landscape (PEL) and is a highly inhomogeneous distribution of peaks and valleys – for which a statistical approach is needed to extract predictions [30]. Physically reasonable but speculative statistical assumptions about the distribution of metastable regions permit a qualitative treatment of the dynamics on the PEL and have yielded useful insights on features like melting (T_m) and diffusion.

An important feature that is not directly derivable from the generic PEL is the particular molecular structures – not even average structures. For these, more specific methods are required. The experiments and theory in the present chapter are primarily concerned with elucidating local structures. The emerging picture of

network glass structures as falling into three distinct mechanically elastic types (or phases), namely, floppy, isostatically rigid (the IP) and stressed rigid are as yet not describable with landscape arguments, particularly, the IP which, like an ordered phase, is not readily located on the PEL. It is hoped that future conceptual progress will enable the PEL picture to delineate (and predict) these mechanical phases.

A new beginning in understanding glasses at a basic level emerged in 1979 when Phillips [31] anticipated that a subtle balance between atomic degrees of freedom and mechanical constraints can arise in covalent networks when they possess optimal connectivity and lead liquids to undergo a glass transition with minimal enthalpic change, i.e., the glass formation tendency (GFT) is optimized. For liquids constrained only by bond-bending and bond-stretching interactions, the number of mechanical constraints per atom (n_c) can be easily computed, and when these match the available degrees of freedom (3) per atom in 3D, one can expect a glass transition with low enthalpic changes to occur. Thus the condition $n_c = 3$, when glasses are optimally constrained, has served as an interesting basis for the search of optimal glass forming compositions.

To see examples of optimally constrained networks leading to facile glass formation, one can examine as a function of composition the minimal liquid cooling rate needed to form a glass or avoid crystallization. In Table 3.1 we show examples of chalcogenides [32] where critical cooling rates show a global minimum in select systems.

Table 3.1. Predicted optimally constrained network compositions and observed minimal critical cooling rate compositions for glass formation.

Glass composition	Ge_xSe_{1-x}	As_xSe_{1-x}	$(1-x)SiO_2-xNa_2O$	$(1-x)SiO_2-xK_2O$
Predicted optimally constrained ($n_c = 3$) network composition 'x'	20%	40%	20%	17%
Observed minimal critical cooling rate composition 'x'	16%	~35%	24%	22%

For the case of the two covalent systems the predicted optimal glass composition ($n_c = 3$) correlates rather well with the location of the minimal cooling rate composition. Phillips' predictions [31] are widely supported by experiments on covalent systems.

Once constraints associated with terminal atoms could be enumerated [33], it became feasible to extend constraint theory to networks containing dangling ends such as halogens in chalcohalide glass systems. The correlation between glass forming tendency and regions of compositions where networks become optimally

constrained (n_c = 3) in the chalcohalides is found to be remarkably impressive [34]. Finally, the interplay between high T_gs and broken bond-bending constraints came to the fore as one began to understand the microscopic origin of the pronounced glass forming tendency of SiO_2 [35]. The hierarchical nature of constraints with strong ones (due to bond-stretching forces) usually intact while weaker ones (due to bond-bending forces) possibly breaking in systems with high T_gs has opened new avenues to extending constraint theory from covalent systems to ionic glasses.

Another factor promoting glass formation, particularly in metallic systems and even modified oxides comes from the variation of η with composition at a fixed T or at the liquidus temperature. Mysen and Richet have suggested [36] that the GFT is increased in systems where a melt viscosity increase can be shifted to low temperatures, such as at eutectics. In the silicates (Table 3.1) optimal glass compositions are close to the prediction of constraint counting algorithms and also to the eutectic compositions (respectively 23% and 19% in modifier composition for sodium and potassium silicates). This suggests that both mechanisms probably contribute to the GFT in these cases.

3.4.1 Compositional Trends of the Glass Transition Temperature

It is well known that an increase of network connectivity (or degree of cross-linking) leads to an increase of T_g. Indeed, liquids with soft interactions such as organic systems are able to more easily equilibrate during quench than liquids with strong interactions such as covalent systems. Energy barriers are small in the former while they are large in the later resulting in low glass transition temperatures in the former but high ones in the latter (T_g = 268K for sorbitol, and T_g = 1450 K for silica). Beyond this very general view, it appears that a detailed study of the behavior of T_g with composition, when measured under standard conditions at a fixed cooling rate, provides insight into the structure of glasses through their network connectivity. In binary and ternary alloy glasses, the observation of an Arrhenius-like increase of viscosity as T approaches T_g is related to covalent bond creation, which can be encoded in local structural units stochastically agglomerating. In the stochastic agglomeration theory (SAT) one seeks a solution of a dynamical master equation [21] in which coordination numbers of the local structural units (such as pyramids, tetrahedral, etc.) and their concentrations are specified, and the solution yields parameter-free predictions of T_g variation with modifier composition. Thus, for example, in binary alloys of the form B_xA_{1-x} (e.g. Ge_xSe_{1-x}), the slope of T_g with x at low modifier concentration (x) becomes [20]:

$$\left[\frac{dT_g}{dx}\right]_{x=0} = \frac{T_g(x=0)}{\ln\left[r_B / r_A\right]} \tag{3.3}$$

where r_B and r_A are the coordination units of the agglomerating species. In Ge_xSe_{1-x}, this slope is for instance T_g $(x = 0)/\ln 2$. These predictions are in remarkable agreement with experimental data on a large class of binary and ternary glass-forming systems including oxides and chalcogenides (see below). Noteworthy is the fact that these predictions fail when the glasses enter the IP regime as the mean coordination number increases to $<r> \sim 2.4$ (see below).

An alternative view [37] to understanding T_g variation with chemical composition is provided by combining rigidity theory (see below) with the Lindemann's melting criterion [38]. Crystals are thought to melt when the thermal mean square displacement $< u^2(T) >$ of atoms acquires 10% of the nearest-neighbor bond length. If the same criterion is applied [39] to highly viscous liquids at T_g, one can obtain the $< u^2(T) >$ by using

$$f = 2 - \frac{5}{6} <r>$$ (3.4)

the floppy mode fraction (f) modified vibrational density of states. The approach provides a statistical physics basis for the empirical Gibbs-DiMarzio [40] equation:

$$T_g = \frac{T_g(<r> = 2)}{1 + B(<r> - 2)}$$ (3.5)

where the parameter B is related to the average floppy mode frequency of the system. This parameter can be also computed from the topology of the network [41]. Measurements of the Lamb-Mössbauer mean square displacements [42] in binary Ge-Se glasses have permitted predicting variations in T_g as a function of network connectivity (see below).

In experimental investigations of glasses variations in physical properties as a function of composition in multi-component systems have proved to be far more incisive than merely focussing on stoichiometric glass compositions. Real glasses do not always possess fully polymerized networks. In several instances networks demix into two or more backbones, i.e., nanoscale phase separate (NSPS) [43]. Such structure information is encoded in the glass composition variation of T_g. For example, the maximum of T_g in binary Ge_xSe_{1-x} glasses near $x \sim 1/3$ is due to NSPS [44, 45], and results because Ge-Ge bonds formed at $x > 0.32$ apparently demix from the network backbone. Such a maximum in T_g is *not observed* in corresponding Si_xSe_{1-x} glasses suggesting that in this case Si-Si bonds formed at $x > 1/3$ apparently *do form part of* the network backbone. Finally, in comparing T_gs of binary Ge_xS_{1-x} glasses with Ge_xSe_{1-x} ones, one finds the ratio to be 1.13 and nearly independent of x once $x > 1/5$. The T_g ratio of 1.13 reflects a chemical bond-strength scaling of glassy networks possessing the same connectivity. We note that

the Pauling [46] single Ge-S bond strength of 55.52 kcal/mole exceeds that of the Ge-Se bond strength of 49.08 kcal/mole by 13%. These ideas permit one to separate the role of chemical bond strengths [47] from network connectivity in determining T_g of glassy systems. Structure information on network *connectivity* accessible from thermal probes complements in a significant way results on glass structure accessible from traditional methods -diffraction and local probes.

3.5 Calorimetric Measurement of the Glass Transition Temperature and Related Thermal Properties

Differential Scanning Calorimetry (DSC) has been traditionally used to measure glass transitions [48] in a wide array of disciplines including food science, pharmaceuticals, and materials science. In a typical experiment, a few tens of milligrams of a sample encapsulated in an Al pan with a lid, and a second identical pan and lid with no sample used as a reference pan, are heated at a fixed scan rate typically of 10°C/min. The difference in heat flow between a sample and a reference displays an endotherm near a glass transition event as a sample softens and atomic mobility increases. We provide in Fig. 3. 3 an example of a DSC scan of a stoichiometric bulk GeSe$_2$ glass.

If the scan rate is lowered from 10°C/min to 3°C/min, the endothermic signal strength decreases by a factor of 3/10 and shifts to a lower temperature. The inflexion point of the endotherm is generally used to define T_g. The lowering of scan rate dT/dt (where t is the time) lowers the signal strength, but it also lowers T_g because of the kinetic nature of the glass transition. The rate of heat flow can be written as,

$$dH/dt = m \, C_p^{\,k} \, (dT/dt) \qquad\qquad (3.6)$$

where H designates the quantity of heat flow to a sample of mass m with a kinetic specific heat $C_p^{\,k}$. To increase dH/dt, it is customary to increase the scan rate (dT/dt). This has the effect of up-shifting glass transition temperatures as well. Such shifts have been used to extract activation energies for enthalpy relaxation near T_g using model descriptions. On the other hand, changes in T_g brought about by those in sample chemistry alone are difficult to isolate using DSC not only due to finite scan rates used but also because the observed heat flow signal has both ergodic and non-ergodic contributions.

Modulated DSC is a more recent variant of DSC [49] and it makes use of a programmed T profile that includes a sinusoidal temperature variation superposed on the linear T-ramp. From the envelope of the modulated heat flow, one obtains the part of the total heat flow that tracks the sinusoidal modulation, and it is called the *reversing* heat flow. The average of the modulated heat flow gives the *total heat flow*, and by subtracting the *reversing heat flow* from the *total heat flow* one

obtains the *non-reversing* heat flow. Fig. 3. 3 shows an m-DSC scan of a similar GeSe$_2$ glass sample taken at 3 °C/min scan rate and a 0.01 °C/s modulation rate.
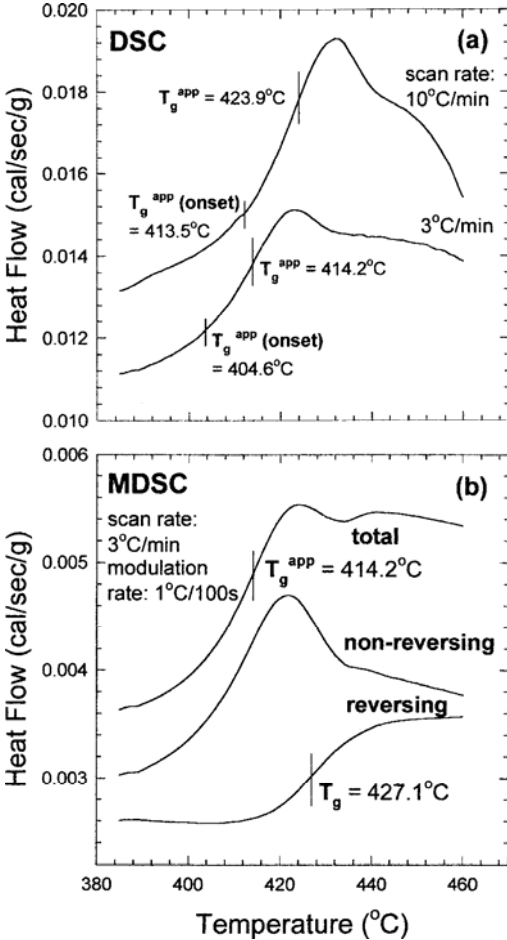
Fig. 3.3 Illustrates in (a) DSC scans of GeSe$_2$ glass taken at 10°C/min and at 3°C / min. and in (b) m-DSC scan of the same sample taken at 3°C / min scan rate and 1°C / 100 s modulation rate [44].

One finds that the total heat flow signal in the m-DSC scan is the same as in the DSC scan (compare Fig. 3. 3a and b). Furthermore, the *reversing* heat flow signal shows a rather clean step, and one extracts the glass transition (T_g) from the inflexion point of the step. From the height of the step one obtains the thermodynamic specific heat difference ΔC_p between the specific heat of the liquid (C_p^l) and the glassy state (C_p^g), $\Delta C_p = C_p^l - C_p^g$ unpolluted from kinetic effects. The *non-reversing* heat flow signal usually displays a Gaussian profile and the integrated

area under the profile yields the *non-reversing enthalpy* (ΔH_{nr}) associated with T_g. Since the $H = H_r + H_{nr}$ where H_r is the reversing and H_{nr} is the non-reversing enthalpy, one can recast, Eq. (3.6) above as,

$$dH/dt = = mC_p dT/dt + dH_{nr}/dt \qquad (3.7)$$

where C_p designates the quasi-thermodynamic specific heat, dH_{nr}/dt the *non-reversing* heat flow, and dH/dt the *total* heat flow term. It is usual to program m-DSC scans for a scan down following a scan up in T across T_g. The difference signal, ΔH_{nr}(up)- ΔH_{nr}(down) = ΔH_{nr} yields the frequency corrected *non-reversing enthalpy* which is independent of the modulation frequency [49]. The AC nature of m-DSC experiments permits phase sensitive detection of signals, resulting in higher sensitivity than possible in a DSC experiment. This has the consequence that m-DSC runs can be undertaken at rather low scan rates (1 °C/min or lower) and even under quasi-static conditions to study glass transitions [49]. For scan rates of 3 °C/min used in our experiments, the typical difference between T_g(up) and T_g(down) is about 2 °C. By taking the mean value of these transitions, one then obtains a scan rate independent T_g. Results on GeSe$_2$ glass reveal T_g = 427(1)°C. m-DSC derived glass transition temperatures thus have made it possible to track changes in T_g brought about by sample composition or on account of sample heterogeneity brought about by incomplete sample processing [50]. Experiments on covalent glasses have shown that aging effects, sample purity (including water traces) and heterogeneity effects are reflected in the non-reversing heat flow term exclusively. The reversing heat flow signal remains largely independent of thermal history including aging and sample purity. Compositional trends in T_g have served a useful role in elucidating the nature of nanoscale phase separation in glasses.

Consider Fig. 3.4 that shows trends in T_g in three covalent systems studied as a function of their mean coordination number <r>. Note that in the two binary As-Se and Ge-Se glasses a global maximum in T_g occurs near <r> ~ 2.4 and <r> ~ 2.67 respectively, the chemical thresholds. On the other hand, in the ternary glass system no T_g maximum is observed even though a chemical threshold exists near <r> ~ 2.55. Homopolar bonds once nucleated in the binary glasses near <r> ~ 2.40 in As-Se and near <r> ~ 2.67 in Ge-Se, apparently segregate from the backbone to form separate nanophases. On the other hand in the ternary glass system homopolar bonds form part of the main backbone [51] and steadily increase network cross-linking as reflected in the almost linear increase of T_g. Ternary Ge$_z$As$_z$Se$_{1-2z}$ glasses are ideal test systems to probe glass forming tendency, nature of glass transitions and the elastic behavior of underlying backbones because their connectivity steadily increases as their chemical composition z is increased.

DSC measurements on DC magnetron sputtered amorphous Ge$_x$Sb$_y$Te$_{1-x-y}$ thin-films at several compositions were investigated by Kalb et al. [52] in both theas deposited (virgin) and thermally annealed state. Although no T_g was observed in the virgin state, these authors could observe a T_g in the thermally
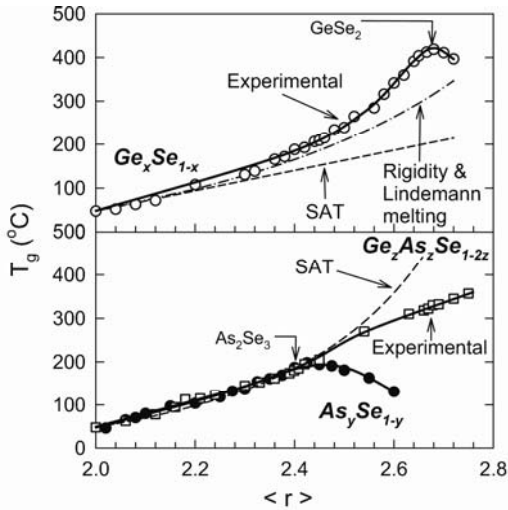
Fig. 3.4. T_g variation in titled chalcogenides with composition [22]. The mean coordination number, $<r> = 2(1 + x)$ for Ge_xSe_{1-x} glasses ($\circ$), $2+y$ for As_ySe_{1-y} glasses ($\bullet$) and $2 + 3z$ for $Ge_zAs_zSe_{1-2z}$ glasses ($\square$). Top panel gives predictions of equ. (3.3), and (3. 5) for Ge_xSe_{1-x}, and bottom panel equ.(3. 3) for the Ge-As-Se ternary. SAT-Stochastic Agglomeration Theory.

annealed state just before crystallization. These experiments on phase change materials highlight the presence of structural relaxation effects in amorphous thin-films.

3.6 Three Generic Classifications of Glasses and Glass Transition Temperatures

The physics of the *glassy state* and specially the nature of *glass transitions* can be elegantly probed using ternary chalcogenide glasses. In such glasses one has the luxury of systematically and reproducibly changing network connectivity (mean coordination number $<r>$) by compositional tuning. These materials are available in rather pure chemical form, and homogeneous bulk glass samples can be synthesized by appropriate handling and processing. The rich database on covalent systems reveals *glass transitions* can be classified into *three distinct* types based on the *elastic behavior* of their underlying backbones.

In the $Ge_xAs_xSe_{1-2x}$ ternary, variation of the non-reversing enthalpy, $\Delta H_{nr}(x)$ reveals [51] three distinct regimes. One observes the enthalpy to show a global minimum (~ 0 cal/g) in the $9\% < x < 16\%$ range, and to increase at $x > 16\%$, and to increase at $x < 9\%$. These three regimes represent respectively at low x ($< 9\%$) the *flexible* phase, at intermediate x ($9\% < x < 16\%$) the *rigid but unstressed phase (IP)*, and at high x ($> 16\%$) the *rigid but stressed phase*. These identifications are further supported by Raman scattering measurements , which reveal vibrational

mode frequency ($v_{CS}(x)$) of corner-sharing tetrahedral Ge(Se$_{1/2}$)$_4$ units to increase with x displaying thresholds at respective phase boundaries (Fig. 3.5a).
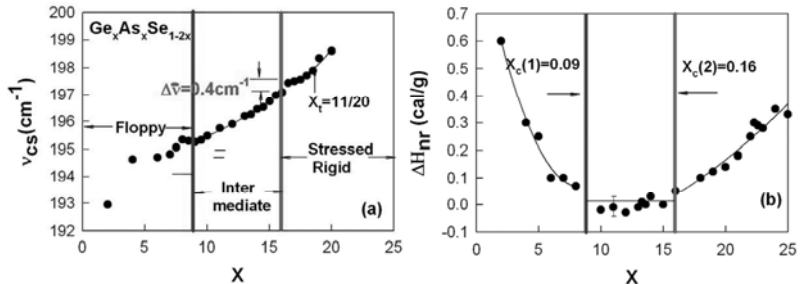
Fig. 3.5. Variations in (a) the frequency of Raman active corner-sharing GeSe$_{(1/2)4}$ units and (b) non-reversing enthalpy near Tg in Ge$_x$As$_x$Se$_{1-2x}$ glasses examined as a function of x. These data reveal three distinct regimes of behavior separated by two elastic phase boundaries; rigidity transition near x = 9% and stress transition near 16%. The figure is taken from ref. [51].

Furthermore, optical elasticity (v_{CS}^2) variation as a function of x displays [53] characteristic power-laws in the intermediate and stressed-rigid phases. The observed elasticity power-law in the stressed-rigid regime is in harmony with numerical predictions [54] based on random network models. The striking correlation between Raman scattering and calorimetric data shown here is observed in several other glasses as well.

In Fig. 3.6, we show m-DSC results on a companion ternary glass system; P$_x$Ge$_x$Se$_{1-2x}$.
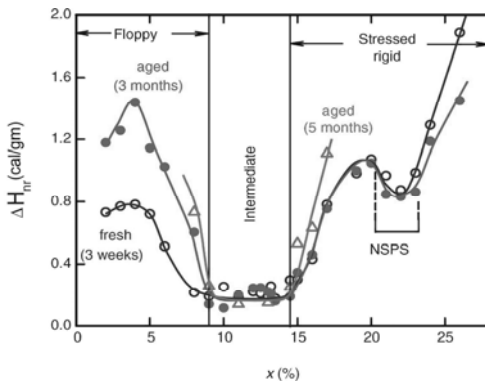
Fig. 3.6. Variation in the non-reversing enthalpy of Ge$_x$P$_x$Se$_{1-2x}$ glasses studied as a function of x in their fresh (○), 3-month aged (●) and 5 month aged (△) state. These data reveal the lack of aging of the enthalpy term in the IP and its presence outside the IP [55]

Perhaps the most striking feature [55] of these data is the minuscule ΔH_{nr} term in the 9% < x < 14.5% range, the IP, and the absence of aging in the IP and the presence of aging for compositions outside the IP, both in the flexible and stressed-

rigid phases. The structure of $P_xGe_xSe_{1-2x}$ ternary differs from that of the As_x Ge_xSe_{1-2x} ternary in one important respect; some of the P atoms segregate in the form of P_4Se_3 molecules as x increases to ~ 20%. In Raman scattering sharp intramolecular stretch modes of the molecule are observed [53]. Segregation of P_4Se_3 molecules leads to some loss of network backbone, and that is reflected in not only the compositional dependence of T_g (x) but also in that of the non-reversing enthalpy (Fig. 3.6).The satellite feature labeled NSPS (Fig. 3.6) is due to nanoscale phase separation of P_4Se_3 molecules. A close examination of the *glass transition endotherm* in the three elastic regimes displays the following characteristic features. In the *elastically flexible* phase, one finds the non-reversing enthalpy at T_g , i.e., ΔH_{nr} term to be generally narrow (~ 20°C wide typically), symmetric and to steadily increase with waiting time in a stretched exponential fashion. In the IP, glass endotherms possess a minuscule ΔH_{nr} term, and the term furthermore does not to age much. In this range glass transitions become *thermally reversing* in character. In the stressed-rigid phase, one finds glass transition endotherms to be wider (~40 °C) , asymmetric with a high-T tail and the heat flow term to age. An example of such a behavior is seen in $GeSe_2$ (Fig. 3.3). Glass transition studies supported by spectroscopic experiments have permitted constructing global phase diagrams, delineating the three phases (see Fig.3.7) for the case of the Ge-P-Se ternary.
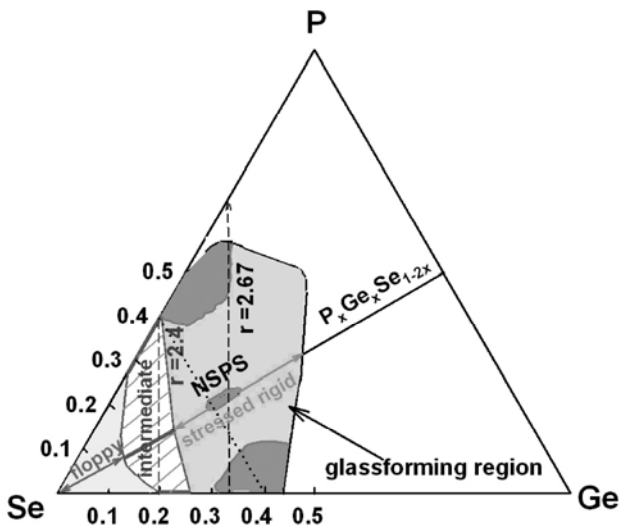
Fig. 3.7. Global Phase diagram of Ge-P-Se ternary illustrating the three elastic phases [53]. Demixing of network backbone near compositions of $GeSe_2$, P_4Se_6 and $P_2Ge_2Se_6$ is reflected by darker grey regions .

Se-rich glasses are flexible because Se-chains dominate the structure of such glasses. Progressive cross-linking of chains of Selenium by P- and Ge- cations leads to the formation of the intermediate phase (hashed region). Increased P- and

Ge- alloying leads next to the formation of stressed-rigid glasses (grey region) in which select regions show a propensity to demix (darker grey regions).

3.7 Elastic Phases in Ionic and Super-ionic Glasses

Recently, the physical properties of ionically bonded network glasses, such as alkali silicates [56] and germanates [57] have been examined in thermal, optical, mechanical measurements. Experiments also reveal that traces of water influence their physical property in significant ways, particularly the non-reversing enthalpy near T_g. In $(Na_2O)_x(GeO_2)_{1-x}$ glasses one finds a wide, sharp and deep reversibility window in the 14% < x < 19% soda range; the composition range defines the *IP*. Glass compositions at x < 14% are in the *stressed-rigid phase* while those at x > 19% are in the *flexible phase*. The stress-free character of glasses in the IP has been strikingly demonstrated in birefringence measurements. Mass densities (molar volumes) reveal a broad maximum (minimum) near x = 18% [58], a result that is identified with the germanate anomaly. The overlapping of the molar volume minimum with the IP suggests that multiscale structural self-organization most likely is responsible for the space filling nature of the IP and that the germanate anomaly is of an elastic origin.

Recently, the molecular structure and thermal properties of the fast-ion conducting glass system, $(AgPO_3)_{1-x}(AgI)_x$ were examined [59] in Raman scattering , infrared reflectance and m-DSC experiments. The thermal measurements show a rather strikingly wide, deep and sharp reversibility window in the 9% < x < 37.8% AgI range. This observation in conjunction with Raman optical elasticity fixes the three elastic phases in this solid electrolyte system, a conclusion similar to the one described above for sodium germanate glasses. In both systems particular care to exclude water [60] in sample synthesis is necessary to observe these intrinsic effects.

3.8 Ideal Glasses and Self-organization of Networks

The minuscule non-reversing enthalpy (ΔH_{nr}) of glass compositions in the thermally reversing window suggests that such glass compositions find themselves configurationally quite close to their liquid counterparts. They can form glasses even when liquids are cooled very slowly since small changes in structure underlie structural arrest. These compositions represent the sweet spots of glass formation. On an entropy plot $S(T)$ (Fig. 3.1) such glasses exist in states characterized by the highest entropy. This is due to the fact that there are multitudes of energetically equivalent global configurations in which such stress-free networks can exist. The stress-free character [13] of such networks was recently demonstrated [61] in Ra-

man pressure experiments on binary Ge-Se glasses. Measurements of mass densities independently show that such glass compositions usually possess form *space filling networks*. Such glass compositions are "*ideal glasses*" and their structures cooperatively adapt to self-organize.

Fig. 3.8 provides a summary of reversibility windows observed in several families of inorganic glasses.
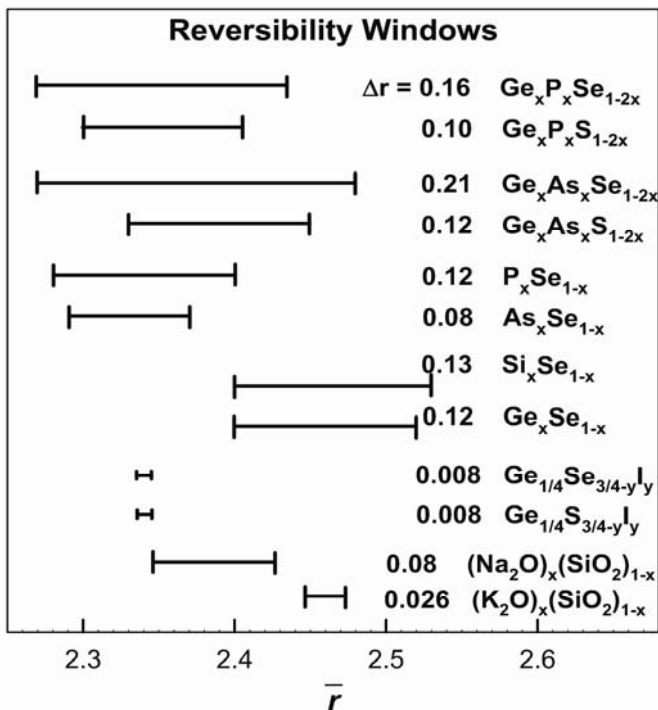

Fig. 3.8. Observed reversibility windows in titled glasses shown as a bar chart in $<r>$-space. Window centroids in group IV selenides are at $<r> > 2.40$, and in group V-selenides at $<r> < 2.40$, while ternary alloys encompass both regions of $<r>$ space.

Here the horizontal bars represent the region in $<r>$ -space over which reversibility windows are manifested in m-DSC experiments. There are aspects of local and intermediate range structure that control centroids and widths of these windows [62]. Glasses of the group IV-selenides have window centroids moved to $<r> > 2.40$, while glasses of the group V- selenides have window centroids moved to $<r> < 2.40$. Ternary alloys comprising of both group IV and V–selenides display much wider windows encompassing both regions. Network structural va-

riance in several forms may be controlling location of IPs, and it is an issue of on-going discussions in the field.

3.9 Does the View Below the Glass Transition Temperature Correlate with the View above the Glass Transition Temperature?

The dynamics of glass forming liquids can be conveniently represented on a plot of log η against $(1/T)$ with the slope near $T = T_g$ providing an activation energy (ΔE_a) for viscosity relaxation (Fig. 3.9).
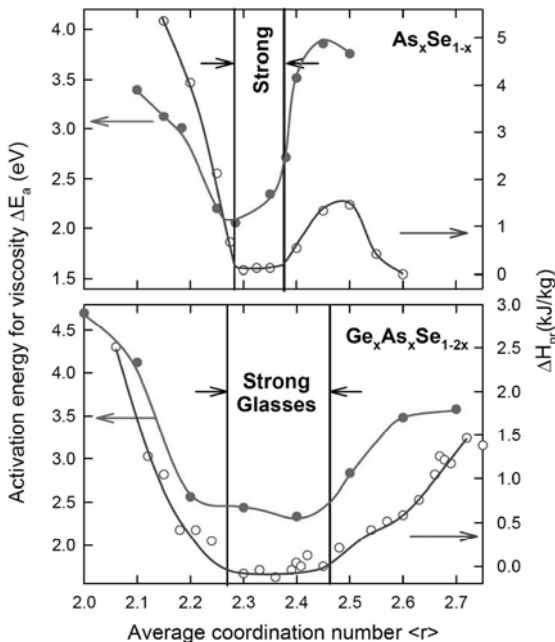
Fig. 3.9. Variations in the activation energy for viscosity ($\bullet$) and non-reversing enthalpy ($\circ$) in (a) binary As_xSe_{1-x} glasses, and (b) ternary $Ge_xAs_xSe_{1-2x}$ glasses as a function of their mean coordination number $<r>$. Global minima in $\Delta H_{nr}(r)$ coincide with a window in ΔE_a for these covalently bonded networks. Figure is taken from [7].

The dimensionless activation energy becomes the fragility (m). Liquids characterized by a smaller ($m \sim 12$) slope show an Arrhenius variation of η and are labeled as *strong* liquids while liquids characterized by a high slope $m > 16$ are labeled as *fragile*. Subsequently, calorimetric, light scattering, dielectric relaxation and shear measurements were brought to bear [63] as measures of liquid fragilities through a measurement of relaxation times τ. Fairly complete viscosity measurements on binary As_xSe_{1-x} and ternary $Ge_xAs_xSe_{1-2x}$ liquids are available in the literature [7].

Compositional trends in $\Delta E_a(x)$, and the non-reversing enthalpies, $\Delta H_{nr}(x)$ of these glasses (Fig. 3.9), reveal that the global minimum in $\Delta E_a(x)$ coincides with that in $\Delta H_{nr}(x)$. These data serve to correlate the *strong-fragile* classification of glass forming *liquids* with the *flexible-intermediate stressed-rigid* classification of corresponding *glasses*. The correlation unequivocally shows that in covalent systems IP glasses give rise to *strong liquids*, while both *flexible and stressed-rigid* glasses give rise to *fragile liquids*. The result unequivocally suggests that in the chemically strongly bonded glasses there are aspects of liquid structure that carry over to the glassy state. Do such correlations exist in other types of networks such as the oxides, superionic solid electrolytes, hydrogen bonded glasses, organic polymers and proteins? We comment on some of these issues next.

3. 10 Glass Formation in Hydrogen Bonded Networks

Several carbohydrates including polyalcohols and saccharides are known to be good glass formers, and their liquid properties such as fragility (m) and stretched exponents (β) and glassy behavior including T_g and Boson peak characteristics have been the subject of earlier work in the field [64]. Their glass transitions have recently been examined in m-DSC experiments [65]. These measurements permit enthalpic relaxation studies to be extended to much lower frequencies than accessible to dielectric studies, and thus approaching T much closer to T_g than hitherto possible. Modulated-DSC results of m and β correlate well with A.C. calorimetric, shear and light scattering measurements. On the other hand dielectric measurements yield m and β parameters that differ noticeably from thermal results [66].

Recently Phillips [10] has extended constraint counting algorithms to H-bonded systems, and has suggested that the remarkably high T_g of trehalose and its bioprotective properties may be the result of a tandem repeat structure of this disaccharide. In this structure weakly and strongly bound glucose rings alternate. His enumeration of constraints suggests that trehalose could represent the case of an optimally constrained network glass if the two gearing constraints associated with torsional motion of the two flaps are intact. We have examined the glass transition in trehalose samples prepared by dehydrating crystalline trehalose dihydrate. Fig. 3.10 gives an m-DSC scan of such a sample and reveals a T_g of 117 °C, and a vanishing (ΔH_{nr} ~0 cal /g) non-reversing enthalpy. The magnitude of ΔH_{nr} places trehalose glass as belonging to an optimally coordinated network, in good agreement with the prediction of Phillips [10]. The fragility of liquid trehalose is rather high, $m = 107$ [65] and it clearly suggests that as $T > T_g$, weak H-bonds (O-H, ~ 3kcal/mole) constraining the tandem repeats must be progressively broken. Thus, in this H-bonded network we have an example of an IP glass that gives rise to a fragile liquid. One can expect a similar circumstance to prevail in all carbo-
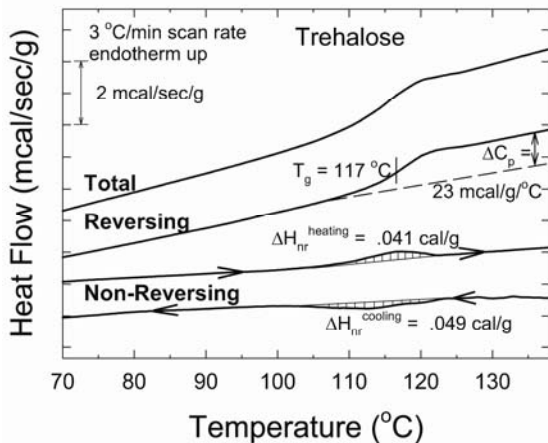
Fig. 3.10. Modulated-DSC scan of trehalose showing a T_g of 117°C, and the heating and cooling non-reversing enthalpies to cancel.

hydrates providing a basis to understand why the fragilities of sugars and alcohols are quite high. In the base oxides such as SiO_2, GeO_2, B_2O_3 composed of network forming cations, one expects their liquids to display a strong behavior ($m \sim 20$); their networks are built of strong chemical bonds and there are no weak links. The situation alters dramatically when the base oxide networks are modified by alkali-oxide additives. Weak alkali atom-non-bridging oxygen ionic bonds form, and as $T > T_g$, these weak links cease to constrain networks, and alkali-atoms mobilities rapidly increase contributing to the fragility. Note that sodium -disilicate and -trisilicate are more fragile than SiO_2 (Fig. 3.2), even though the trisilicate composition is near the IP. In general, in the modified oxides as in the H-bonded systems, one does not expect the glass-liquid correlation to uphold as in the chalcogenides (Fig. 3.9). In the case of the covalently bonded networks such as $Ge_{14}As_{14}Se_{72}$ there are no weak bonds, and one expects this IP glass to give rise to a strong liquid as is found to be the case (Fig. 3.9) and as discussed earlier in section 3.9. Finally, presence of weak H-bonds in Trehalose gives rise to a rather large and measurable temperature change in the specific heat (dC_p/dT) in the glassy ($T < T_g$) as well as in the liquid state ($T > T_g$) of about 1 mcal/gm/°C^2 . The dC_p/dT term is fixed by the slope of the reversing heat flow signal (Fig .3.10). In covalent glasses the dC_p/dT term in the glassy and liquid states are lower by about an order of magnitude than the value obtained here for Trehalose, which is as it should be. The temperature variation of vibrational entropy in a H-bonded network can be expected to be larger than in a covalently bonded one.

3.11 Epilogue

Experiments supported by theory have shown that network glasses broadly exist in *three* generic elastic phases: *flexible*, *intermediate* and *stressed-rigid*, which are determined by the connectivity of their backbones. *IP glasses* are composed of rigid but unstressed networks that are in a state of *quasi-equilibrium* and do not age much. They form space filling networks that are neither random, nor crystalline, but their structures adapt to expel stress and to become *self-organized*. Understanding the structure of IPs in real glasses is an exciting but challenging problem. Multi-scale structural adaption leading to self-organization is an exponentially complex problem. And resolution of the problem will undoubtedly impact basic understanding of the disordered state of matter with consequences on protein folding, and engineering applications of these materials in a variety of existing and evolving technologies.

References

[1] Zachariasen, W.H.: The atomic arrangement in a glass. J. Am. Chem. Soc. **54**, 3841-3851 (1932)
[2] Lucovsky, G., Baker, D.A., Paesler, M.A. and Phillips, J.C.: Spectroscopic and electrical detection of intermediate phases and chemical bonding self-organizations in (i) dielectric films for semiconductor devices, and (ii) chalcogenide alloys for optical memory devices. J. Non-Cryst. Solids **353**, 1713-1722 (2007)
[3] Matthews, J.N.A.: Semiconductor Industry Switches to Hafnium-Based Transistors. Physics Today **61**, 25-26 (2008)
[4] Macfarlane, A. and Martin, G.: Glass : a world history. University of Chicago Press, Chicago (2002)
[5] Kerner, R. and Phillips, J.C.: Quantitative principles of silicate glass chemistry. Solid State Commun. **117**, 47-51 (2000)
[6] Selvanathan, D., Bresser, W.J. and Boolchand, P.: Stiffness transitions in Si_xSe_{1-x} glasses from Raman scattering and temperature-modulated differential scanning calorimetry. Phys. Rev. B **61**, 15061-15076 (2000)
[7] Boolchand, P., Lucovsky, G., Phillips, J.C. and Thorpe, M.F.: Self-organization and the physics of glassy networks. Phil. Mag. **85**, 3823-3838 (2005)
[8] Barre, J., Bishop, A.R., Lookman, T. and Saxena, A.: Adaptability and "intermediate phase" in randomly connected networks. Phys. Rev. Lett. **94**, 208701-4 (2005)
[9] Phillips, J.C.: Universal intermediate phases of dilute electronic and molecular glasses. Phys. Rev. Lett. **88**, 216401-4 (2002)
[10] Phillips, J.C.: Ideally glassy hydrogen-bonded networks. Phys. Rev. B **73**, 024210-10 (2006)

[11] Rader, A.J., Hespenheide, B.M., Kuhn, L.A. and Thorpe, M.F.: Protein unfolding: Rigidity lost. Proceedings of the National Academy of Sciences of the United States of America **99**, 3540-3545 (2002)

[12] Boolchand, P., Georgiev, D.G. and Goodman, B.: Discovery of the intermediate phase in chalcogenide glasses. J. Optoelectron. Adv. Mater. **3**, 703-720 (2001); Micoulaut, M. and Phillips, J.C.: Onset of rigidity in glasses: From random to self-organized networks. J. Non-Cryst. Solids **353**, 1732-1740 (2007); Brière, M.A., Chubynsky, M.V. and Mousseau, N.: Self-organized criticality in the intermediate phase of rigidity percolation. Phys. Rev. E **75**, 56108 (2007)

[13] Thorpe, M.F., Jacobs, D.J., Chubynsky, M.V. and Phillips, J.C.: Self-organization in network glasses. J. Non-Cryst. Solids **266**, 859-866 (2000)

[14] Ovshinsky, S.R.: Reversible Electrical Switching Phenomena in Disordered Structures. Phys. Rev. Lett. **21**, 1450–1453 (1968)

[15] Yamada, N., Ohno, E., Nishiuchi, K., Akahira, N. and Takao, M.: Rapid-phase transitions of GeTe-Sb_2Te_3 pseudobinary amorphous thin films for an optical disk memory. J. Appl. Phys. **69**, 2849-2856 (1991)

[16] Kolobov, A.V., Fons, P., Frenkel, A.I., Ankudinov, A.L., Tominaga, J. and Uruga, T.: Understanding the phase-change mechanism of rewritable optical media. Nature Materials **3**, 703–708 (2004); Baker, D.A., Paesler, M.A., Lucovsky, G., Agarwal, S.C. and Taylor, P.C.: Application of Bond Constraint Theory to the Switchable Optical Memory Material $Ge_2Sb_2Te_5$. Phys. Rev. Lett. **96**, 255501-3 (2006); Wuttig, M.: Phase-change materials: Towards a universal memory? Nat Mater **4**, 265-266 (2005); Lankhorst, M.H.R., Ketelaars, B.W.S.M.M. and Wolters, R.A.M.: Low-cost and nanoscale non-volatile memory concept for future silicon chips. Nat Mater **4**, 347-352 (2005)

[17] Kauzmann, W.: The Nature of the Glassy State and the Behavior of Liquids at Low Temperatures. Chem. Rev. **43**, 219-256 (1948)

[18] Debenedetti, P.G. and Stillinger, F.H.: Supercooled liquids and the glass transition. Nature **410**, 259-267 (2001)

[19] Angell, C.A., Ngai, K.L., McKenna, G.B., McMillan, P.F. and Martin, S.W.: Relaxation in glassforming liquids and amorphous solids. J. Appl. Phys. **88**, 3113-3157 (2000)

[20] Kerner, R. and Micoulaut, M.: On the glass transition temperature in covalent glasses. J. Non-Cryst. Solids **210**, 298-305 (1997)

[21] Micoulaut, M.: The slope equations: A universal relationship between local structure and glass transition temperature. European Physical Journal B **1**, 277-294 (1998)

[22] Boolchand, P., Georgiev, D.G. and Micoulaut, M.: Nature of glass transition in chalcogenides. J. Optoelectron. Adv. Mater. **4**, 823-836 (2002)

[23] Anderson, P.W.: Through the Glass Lightly. Science **267**, 1615-e-1616 (1995)

[24] Binder, K. and Kob, W.: Glassy Materials And Disordered Solids, An Introduction to Their Statistical Mechanics. World Scientific, Singapore (2005)

[25] Tammann, G. and Hesse, W.: Die Abhängigkeit der Viscosität von der Temperatur bie unterkühlten Flüssigkeiten. Z. Anorg. Allg. Chem. **156**, 245-257 (1926); Fulcher, G.S.: Analysis of recent measurements of the viscosity of glasses. J. Am. Ceram. Soc. **8**, 339-355 (1925); Vogel, H.: Physik. Zeitschrift **22**, 645-646 (1921)

[26] Angell, C.A.: Structural Instability and Relaxation in Liquid and Glassy Phases near the Fragile Liquid Limit. J. Non-Cryst. Solids **102**, 205-221 (1988)

[27] Cugliandolo, L.F.: Dynamics of glassy systems. arXiv:cond-mat/0210312v2 (2002)

[28] O'Hern, C.S., Langer, S.A., Liu, A.J. and Nagel, S.R.: Force Distributions near Jamming and Glass Transitions. Phys. Rev. Lett. **86**, 111-114 (2001)

[29] Langer, S.A. and Liu, A.J.: Sheared foam as a supercooled liquid? EPL (Europhysics Letters) **49**, 68-74 (2000)

[30] Giovambattista, N., Stanley, H.E. and Sciortino, F.: Potential-Energy Landscape Study of the Amorphous-Amorphous Transformation in H_2O. Phys. Rev. Lett. **91**, 115504-4 (2003); Angell, C.A.: Glass formation and the nature of the glass transitions. In: Boolchand, P. (ed.) Insulating and Semiconducting Glasses, pp. 1-51. World Scientific, Singapore; River Edge,

NJ (2000); Stillinger, F.H.: A Topographic View of Supercooled Liquids and Glass Formation. Science **267**, 1935-1939 (1995)

[31] Phillips, J.C.: Topology of covalent non-crystalline solids I: Short-range order in chalcogenide alloys. J. Non-Cryst. Solids **34**, 153-181 (1979)

[32] Azoulay, R., Thibierge, H. and Brenac, A.: Devitrification characteristics of Ge_xSe_{1-x} glasses. J. Non-Cryst. Solids **18**, 33-53 (1975); Fang, C.-Y., Yinnon, H., Uhlmann, D.R.: A kinetic treatment of glass formation. VIII: Critical cooling rates for Na_2O-SiO_2 and K_2O-SiO_2 glasses. J. Non-Cryst. Solids **57**, 465-471 (1983)

[33] Boolchand, P. and Thorpe, M.F.: Glass-Forming Tendency, Percolation of Rigidity, and Onefold-Coordinated Atoms in Covalent Networks. Phys. Rev. B **50**, 10366-10368 (1994)

[34] Mitkova, M. and Boolchand, P.: Microscopic origin of the glass forming tendency in chalcohalides and constraint theory. J. Non-Cryst. Solids **240**, 1-21 (1998)

[35] Zhang, M. and Boolchand, P.: The Central Role of Broken Bond-Bending Constraints in Promoting Glass-Formation in the Oxides. Science **266**, 1355-1357 (1994)

[36] Mysen, B. and Richet, P.: Silicate glasses and melts: properties and structure. Elsevier, Amsterdam; Boston (2005); Richet, P.: Viscosity and Configurational Entropy of Silicate Melts. Geochim. Cosmochim. Acta **48**, 471-483 (1984)

[37] Naumis, G.G.: Variation of the glass transition temperature with rigidity and chemical composition. Phys. Rev. B **73**, 172202-4 (2006)

[38] Tabor, D.: Gases, liquids, and solids : and other states of matter. Cambridge University Press, Cambridge; New York (1991)

[39] Phillips, W.A., Buchenau, U., Nücker, N., Dianoux, A.J., Petry, W.: Dynamics of glassy and liquid selenium. Phys. Rev. Lett. **63**, 2381 (1989)

[40] Gibbs, J.H. and DiMarzio, E.A.: Nature of the Glass Transition and the Glassy State. J. Chem. Phys. **28**, 373-383 (1958)

[41] Micoulaut, M. and Naumis, G.G.: Glass transition temperature variation, cross-linking and structure in network glasses: A stochastic approach. Europhys. Lett. **47**, 568-574 (1999)

[42] Boolchand, P., Bresser, W., Zhang, M., Wu, Y., Wells, J. and Enzweiler, R.N.: Lamb-Mössbauer Factors as a Local Probe of Floppy Modes in Network Glasses. J. Non-Cryst. Solids **182**, 143-154 (1995)

[43] Boolchand, P., Georgiev, D.G., Qu, T., Wang, F., Cai, L.C. and Chakravarty, S.: Nanoscale phase separation effects near <r>=2.4 and 2.67, and rigidity transitions in chalcogenide glasses. Comptes Rendus Chimie **5**, 713-724 (2002)

[44] Boolchand, P. and Bresser, W.J.: The structural origin of broken chemical order in $GeSe_2$. Phil. Mag. B **80**, 1757-1772 (2000)

[45] Boolchand, P.: The maximum in glass transition temperature (T_g) near x = 1/3 in Ge_xSe_{1-x} glasses. Asian J. of Phys. **9**, 709 (2000)

[46] Pauling, L.: The Nature of the Chemical Bond. Cornell University, Ithaca, NY (1960)

[47] Tichý, L. and Tichá, H.: Covalent bond approach to the glass-transition temperature of chalcogenide glasses. J. Non-Cryst. Solids **189**, 141-146 (1995)

[48] Wunderlich, B.: The tribulations and successes on the road from DSC to TMDSC in the 20th century the prospects for the 21st century. J. Therm. Anal. Calorim. **78**, 7-31 (2004)

[49] Thomas, L.C.: Modulated DSC Technology (MSDC-2006). T.A. Instruments, Inc (www.tainstruments.com), New Castle, DE (2006)

[50] Cai, L.C. and Boolchand, P.: Nanoscale phase separation of GeS_2 glass. Phil. Mag. B **82**, 1649-1657 (2002)

[51] Qu, T., Georgiev, D.G., Boolchand, P. and Micoulaut, M.: The intermediate phase in ternary $Ge_xAs_xSe_{1-2x}$ glasses. In: Egami, T., Greer, A.L., Inoue, A., Ranganathan, S. (eds.) Supercooled Liquids, Glass Transition and Bulk Metallic Glasses, p. 157. Materials Research Society (2003)

[52] Kalb, J.A., Wuttig, M. and Spaepen, F.: Calorimetric measurements of structural relaxation and glass transition temperatures in sputtered films of amorphous Te alloys used for phase change recording. J. Mater. Res. **22**, 748-754 (2007)

[53] Boolchand, P., Jin, M., Novita, D.I. and Chakravarty, S.: Raman scattering as a probe of intermediate phases in glassy networks. Journal of Raman Spectroscopy **38**, 660-672 (2007)

[54] He, H. and Thorpe, M.F.: Elastic Properties of Glasses. Phys. Rev. Lett. **54**, 2107-2110 (1985)

[55] Chakravarty, S., Georgiev, D.G., Boolchand, P. and Micoulaut, M.: Ageing, fragility and the reversibility window in bulk alloy glasses. J. Phys. Condens. Matter **17**, L1-L7 (2005)

[56] Vaills, Y., Qu, T., Micoulaut, M., Chaimbault, F. and Boolchand, P.: Direct evidence of rigidity loss and self-organization in silicate glasses. J. Phys. Condens. Matter **17**, 4889-4896 (2005)

[57] Rompicharla, V., Novita, D.I., Chen, P., Boolchand, P., Micoulaut, M. and Huff, W.: Abrupt boundaries of intermediate phases and space filling in oxide glasses. J. Physics Condensed Matter **20**, 202101(5pp) (2008).

[58] Henderson, G.S.: The Germanate Anomaly: What do we know? J. Non-Cryst. Solids **353**, 1695-1704 (2007)

[59] Novita, D.I., Boolchand, P., Malki, M. and Micoulaut, M.: Fast-ion conduction and flexibility of glassy networks. Phys. Rev. Lett. **98**, 195501-4 (2007)

[60] Novita, D.I. and Boolchand, P.: Synthesis and structural characterization of dry $AgPO_3$ glass by Raman scattering, infrared reflectance, and modulated differential scanning calorimetry. Phys. Rev. B **76**, 184205-12 (2007)

[61] Wang, F., Mamedov, S., Boolchand, P., Goodman, B. and Chandrasekhar, M.: Pressure Raman effects and internal stress in network glasses. Phys. Rev. B **71**, 174201-8 (2005)

[62] Micoulaut, M. and Phillips, J.C.: Rings and rigidity transitions in network glasses. Phys. Rev. B **67**, 104204-9 (2003)

[63] Carpentier, L., Desprez, S. and Descamps, M.: From strong to fragile glass- forming systems: a temperature modulated differential scanning calorimetry investigation. Phase Transitions **76**, 787 - 799 (2003)

[64] Sokolov, A.P., Rössler, E., Kisliuk, A. and Quitmann, D.: Dynamics of strong and fragile glass formers: Differences and correlation with low-temperature properties. Phys. Rev. Lett. **71**, 2062-2065 (1993)

[65] DeGusseme, A., Carpentier, L., Willart, J.F. and Descamps, M.: Molecular Mobility in Supercooled Trehalose. J. Phys. Chem. B **107**, 10879-10886 (2003)

[66] Macdonald, J.R. and Phillips, J.C.: Topological derivation of shape exponents for stretched exponential relaxation. J. Chem. Phys. **122**, 074510-074510 (2005)